Journal of the Korean Society of Marine Engineering, Vol. 34, No. 7, pp. 997~1008, 2010(ISSN 1226-9549)

Mooring Tension and Motion Characteristics of a Floating Fish Reef with Pipe in Waves and Currents Using Numerical Model

Tae-Ho Kim†

(Received February 24, 2010; Revised July 2, 2010; Accepted July 2, 2010)

Abstract: The mooring line tension and motion response of a floating fish reef system were analyzed using a Morison equation type numerical model. The reef structure was constructed with pipe and suspended up from the bottom with a single, high tension mooring. Input forcing parameters into the model consisted of both regular and random waves, with and without currents. Heave, surge and pitch dynamic calculations were made, along with the tension response in the mooring lines. Results were analyzed in both the time and frequency domains and where appropriate, linear transfer functions were calculated. In addition, damped and natural periods of the system were determined to examine a resonating situation.

Key words: Submerged reef, Morison equation, Transfer function, Natural periods

1. Introduction

Fisheries production in the Korean coastal zones has recently decreased due to over fishing, marine pollution, land reclamation and so forth. In addition, the proclamation of 200-mile Exclusive Economic Zones by many nations has made long-range fishing more difficult.

Therefore, the need for artificial reefs to increase productivity in the coastal waters has greatly increased in Korea. Many artificial reefs have been installed in the Korean waters since the 1970's. By 2008, reefs were installed at 12,634 sites, totaling to a volume of about 10,107,505 m^3[1]. As the most of artificial reefs in Korea are gravity reefs (e.g. dice reef) that have little effect on attracting migratory fishes, another fishing reef(e.g. floating artificial reef) technology has been needed for the enhancement of fisheries productivity.

The floating fish reef is a kind of fishing tool to attract migratory fishes like tuna, yellow tail, slimy mackerel and so on[2]. Because a floating reef system is mainly established in open sea, it is subjected to the external forces from high waves and strong currents. Thus, the system is conservatively designed to withstand environmental loads under waves and currents. In this study, a numerical model study is conducted to investigate the dynamics of a submerged artificial reef system. The reef system is moored by a single, tensioned line. The main component of the system is comprised mostly of pipe. In this study, the reef system is analyzed with a numerical

† Corresponding Author(School of Marine Technology, Chonnam National University, E-mail: kimth@chonnam.ac.kr, Tel: 061-659-3121)

model. The numerical model uses the Finite Element Analysis approach described by Tsukrov et al.[3-4]. The model has been used mostly with open ocean aquaculture type structures, but it is applicable for moored artificial reef systems as well. The results of past model simulations have compared well with both physical model tests and field measurements for a variety of mooring configurations and conditions[5-9]. In addition, a summary of many of the numerical modeling case studies can be found in Fredriksson et al.[10]. Though the results of the model should only be considered approximate, insight can be gained regarding the tension in mooring components and the motion response of the submerged structure.

The objectives of this study are to determine the mooring line tension and motion characteristics of a floating fish reef system with pipe in response to both regular and irregular waves with and without a superimposed current. Numerical models were constructed, simulations were performed and responses were obtained.

2. Materials and methods

2.1 Construction of a floating fish reef with pipe

The reef system analyzed consisted of a subsurface pipe structure. A detailed schematic is shown on Figure 1. Table 1 shows the component details of the reef system.

2.2 Numerical model

2.2.1 Background

Numerical model simulations were performed using the finite element computer program developed specifically for marine aquaculture applications. Wave and current loadings on truss and buoy elements were introduced by utilizing the Morison equation[11]. The algorithm employs a nonlinear Lagrangian formulation to account for large displacements of structural elements. In addition, the unconditionally stable Newmark direct integration scheme is adopted to solve the nonlinear equations of motion. Hydrodynamic forces on the structural elements are calculated using the Morison equation modified to account for relative motion between the structural element and the surrounding fluid as described by Haritos and He[12].

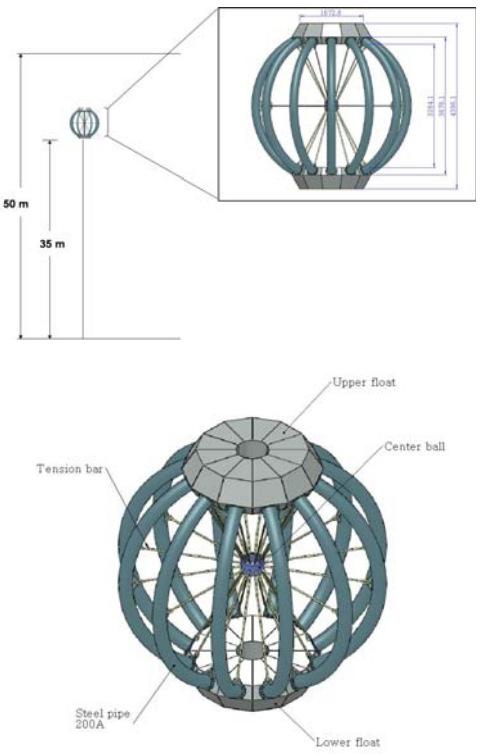

Figure 1: Construction details of the pipe reef system.

2.2.2 Material and geometric properties

The model was built using the material and geometric properties provided in Table 2. This model consisted of 158 nodes and 557 elements. The model is shown in detail on Figure 2. The total system weight and buoyancy were calculated to be 29.9 and 48.6 kN, respectively. Note that these values do not take into account lines, only the major structural components, since they were used as a check versus numerical predictions.

Table 1: Primary components of the pipe reef system.

Component	Parameter	Values
Float	Material	Stainless steel
	Diameter	2085 mm
	Height	556 mm
Pipe	Material	Steel
	Diameter	216.3 mm
	Radius of curvature	1891 mm
Tension rod	Material	Stainless steel
	Diameter	22 mm
	Length	1723 mm
Center ball	Material	Stainless steel
	Diameter	355 mm
	Height	275 mm
Bridle line	Material	Polypropylene
	Diameter	22 mm
Mooring line	Material	Polypropylene
	Diameter	40 mm
	Length	35 m
	Material	Polypropylene rope

Table 2: Geometric and material properties of the pipe reef system

Component	Parameter	Values
Pipe	Density	1025 kg/m^3
	Modulus of elasticity	2.0×10^{11} Pa
	Cross sectional area	0.037 m^2
Float(Top)	Density	321.6 kg/m^3
	Modulus of elasticity	2.0×10^{11} Pa
	Cross sectional area	0.636 m^2
Float(Side)	Density	321.6 kg/m^3
	Modulus of elasticity	2.0×10^{11} Pa
	Cross sectional area	0.196 m^2
Tension rod	Density	7482 kg/m^3
	Modulus of elasticity	1.94×10^{10} Pa
	Cross sectional area	3.434×10^{-4} m^2
Center ball	Density	2180 kg/m^3
	Modulus of elasticity	1.94×10^{10} Pa
	Cross sectional area	0.099 m^2
Bridle line	Density	932.7 kg/m^3
	Modulus of elasticity	3.38×10^{8} Pa
	Cross sectional area	3.801×10^{-4} m^2
Mooring line	Density	932.7 kg/m^3
	Modulus of elasticity	3.18×10^{8} Pa
	Cross sectional area	1.257×10^{-3} m^2
Stiffener (1 & 2)	Density	1025 kg/m^3
	Modulus of elasticity	2.5×10^{11} Pa
	Cross sectional area	5.00×10^{-6} m^2

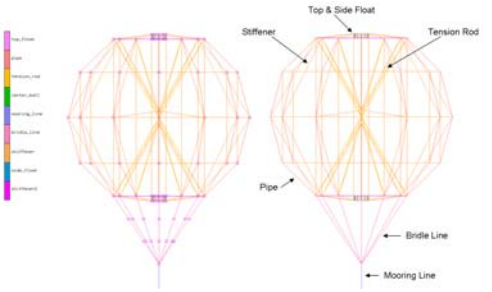

Figure 2: Pipe reef system consisted of 158 nodes and 557 elements.

2.2.3 Input parameters

Once the models were constructed, the first set of tests conducted with the pipe reef system was performed with no forcing so that the static characteristics could be verified. The next set of tests was performed with the numerical model in regular waves with and without the 1.0 m/sec current. The currents were oriented in the same direction as the waves. Each of the load case characteristics are provided in Table 3.

Table 3: Wave and current parameters for each load case.

Load case	Waves		Current (m/sec)
	Height (m)	Period (sec)	
1	2	6	0
2	4	8	0
3	6	10	0
4	8	12	0
5(static)	0	0	0
6	2	6	1.0
7	4	8	1.0
8	6	10	1.0
9	8	12	1.0

To obtain an irregular wave profile in the numerical routine, a spectrum was decomposed into multiple frequency components. The spectrum chosen was a form of the Joint North Sea Wave Project(JONSWAP) spectrum[13] described by

$$S(f) = \alpha H_s^2 T_p^{-4} f^{-5} \exp[-1.25(T_p f)^{-4}]\gamma^Y, \quad (1)$$

where

$$Y = e^{[-(T_p f - 1)^2/2\sigma^2]},$$

$$\alpha = \frac{0.0624}{0.23 + 0.0336\gamma - 0.185(1.9+\gamma)^{-1}},$$

and

$$\sigma = \frac{\sigma_a : f \le f_p}{\sigma_b : f \ge f_p},$$

and f_p is the frequency at the spectral peak($1/T_p$). Parameters γ and σ are used to adjust the height and width of the peak of the curve, respectively. In this study, the default shaping parameters are used and are provided in Table 4, along with H_s of 8.64 m and T_p of 12.73 sec, which were chosen according to a design wave condition of the southern sea of Korea for 20-year return periods[14].

Table 4: JONSWAP parameters used to shape the input spectrum.

Parameter	Values
H_s(m)	8.64
T_p(sec)	12.73
γ	3.3
Power off	-5
σa	0.07
σb	0.09

2.2.4 Motion response locations

For each simulation, motion data sets were acquired to characterize the dynamics of the submerged reef structure. Six "nodes" were chosen for which

horizontal and vertical movements were analyzed:

① Nodes 1 and 2 were positioned on top of the reef structure

② Nodes 3 and 4 were positioned in the middle of the reef structure

③ Nodes 5 and 6 were positioned at the bottom of the reef structure

Tension was acquired at the point where the mooring connects with the seafloor. A schematic is shown in Figure 3.

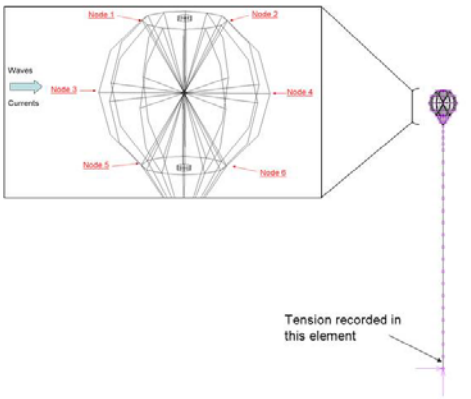

Figure 3: Schematic of the node locations where the motion and tension data were analyzed.

2.3 Data analysis

Regular wave tests were conducted using the numerical modeling for the load cases provided in Table 3. The characteristics of these waves were approximated using linear wave theory characterized by the following velocity potential (ϕ),

$$\phi = -A\frac{g}{2\pi f}\frac{\cosh k(d+z)}{\cosh kd}\sin(kx-2\pi ft), \quad (2)$$

surface elevation(η),

$$\eta = A\cos(kx-2\pi ft), \quad (3)$$

and dispersion relation,

$$(2\pi f)^2 = gk\tan(kd), \quad (4)$$

where A is the wave amplitude(equal to $\frac{1}{2}$ the wave height), g is the gravitational constant, f is the frequency, k is the wave number equal to $2\pi/L$, L is the wave length, d is the water depth, z is the vertical position in the water column and x is the horizontal position.

Linear transfer function magnitudes calculated for deterministic waves, referred to as response amplitude operators(RAOs), are obtained by dividing the amplitude of the response by the amplitude of the force for each wave frequency. The heave, surge, pitch and mooring line tension RAOs are defined as,

① Heave RAO: heave amplitude/wave elevation amplitude,

② Surge RAO: surge amplitude/wave excursion amplitude,

③ Pitch RAO: pitch amplitude/wave slope amplitude and

④ Mooring line tension RAO: Mooring line tension amplitude/wave elevation amplitude.

The wave excursion amplitude(ζ) is defined as the horizontal semi-axis of the ellipse formed by the water particle trajectory(at the surface). It is found by taking the partial derivative of equation (2) with respect to x to obtain the horizontal velocity component. Integrating this result with respect to time(t), and dropping the oscillating term, gives the wave excursion amplitude

$$\zeta = A\frac{\cosh kd}{\sinh kd}. \quad (5)$$

The wave slope amplitude(Θ) is obtained by taking the partial derivative of equation (3) with respect to x and

dropping the oscillating term,

$$\theta = kA. \quad (6)$$

The resulting wave characteristics for each of the load cases are provided in Table 5. In the Table, the wave number(k) is obtained by solving the dispersion relation(Equation 4) and the wave excursion and slope amplitude from equations (5) and (6), respectively.

Table 5: Calculated wave particulars for each load case without the influence of the currents.

Load case	A (m)	L (m)	k (rad/m)	ζ (m)	Θ (rad)
1 & 6	1	56	0.1122	1.00	0.1122
2 & 7	2	100	0.0628	2.01	0.1257
3 & 8	3	151	0.0416	3.10	0.1248
4 & 9	4	205	0.0306	4.39	0.1226
5	-	-	-	-	-

2.4 Irregular wave tests

Numerical model tests were also conducted using irregular waves. Irregular waves(and the system response) are described by a spectrum in the frequency domain in terms of units proportional to energy per frequency band. The wave elevation auto-spectrum is typically described by the significant wave height and the dominant wave period. Statistically the significant wave height is often estimated from H_{mo} and is calculated from the zeroth moment of the spectrum,

$$m_j = \int_0^\infty f^j G(f) df, \ \ where\, j = 0 \ldots n, \quad (7)$$

in the case where j=0 and G(f) is the one sided wave elevation auto-spectral density. The zeroth moment of the spectrum is also the area under the spectral curve equal to the variance. If the spectrum is narrow banded and the wave heights follow a Rayleigh probability distribution[15], H_{mo} is obtained from,

$$H_{mo} = \sqrt[4]{m_o}. \quad (8)$$

In deep water, H_{mo} is approximately equal to the average of the top third wave heights[16], which is the significant wave height(H_s) used in the JONSWAP spectrum. The dominant wave period, T_p, is one over the frequency at which the maximum energy in a spectrum occurs. The wave elevation auto-spectrum is calculated from the measured times series using a discrete form of

$$S_{xx}(f) = \underset{T\to\infty}{\mathrm{Lim}} \frac{1}{2T} X(f) X^*(f), \quad (9)$$

where $S_{xx}(f)$ is the two sided, auto-spectral density function, $X^*(f)$ is the complex conjugate of $X(f)$ and T is the record length. The two sided auto-spectral density function is continuous for all frequencies between $-\infty$ and ∞. In standard observational practice, however, the one sided auto-spectral density function, $G_{xx}(f)$, is used, where

$$G_{xx}(f) = 2S_{xx}(f) \quad 0 \le f \le \infty, \quad (10)$$

Note that $G_{xx}(f)$ could be the same term used in equation (2). For the irregular wave simulations, linear transfer functions were calculated as a function of frequency using auto- and cross-spectral methods. In the frequency domain, the system force can be described in terms of energy density as $G_{\eta\eta}(f)$ that is wave elevation auto-spectrum(m^2/Hz), $G_{\zeta\zeta}(f)$ that is wave excursion auto-spectrum

(m^2/Hz), and $G_{\Theta\Theta}(f)$ that is wave slope auto-spectrum(rad^2/Hz). The wave excursion and slope auto-spectra are calculated from the wave elevation auto-spectrum using the following relationships,

$$G_{\zeta\zeta}(f) = G_{nn}(f) \cdot [\tanh(kd)]^{-2} \quad (11)$$

and

$$G_{\theta\theta}(f) = G_{\eta\eta}(f) \cdot (k)^2, \quad (12)$$

respectively, where k=k(f) according to the dispersion relation.

Likewise, the auto-spectral motion response in heave, surge, pitch and tension response in the mooring line are calculated using that $G_{hh}(f)$ is heave response auto-spectrum(m^2/Hz), $G_{ss}(f)$ that is surge response auto-spectrum(m^2/Hz), $G_{pp}(f)$ that is pitch response auto-spectrum (rad^2/Hz) and $G_{tt}(f)$ that is mooring element tension response auto-spectrum (kN^2/Hz).

To obtain the linear transfer function using the auto-spectral technique between the force and the response, the following calculations are made,

$$|H_{hh}(f)| = \left[\frac{G_{hh}(f)}{G_{\eta\eta}(f)}\right]^{\frac{1}{2}} \quad (13)$$

$$|H_{ss}(f)| = \left[\frac{G_{ss}(f)}{G_{\zeta\zeta}(f)}\right]^{\frac{1}{2}} \quad (14)$$

$$|H_{pp}(f)| = \left[\frac{G_{pp}(f)}{G_{\theta\theta}(f)}\right]^{\frac{1}{2}} \quad (15)$$

$$|H_{tt}(f)| = \left[\frac{G_{tt}(f)}{G_{\eta\eta}(f)}\right]^{\frac{1}{2}} \quad (16)$$

where $H_{hh}(f)$ is the heave transfer function, $H_{ss}(f)$ is the surge transfer function, $H_{pp}(f)$ is the pitch transfer function and $H_{tt}(f)$ is the mooring element tension transfer function.

3. Results and discussion

3.1 Hydrostatic analysis

The first set of numerical model simulations were performed without current and wave loading. In each of the simulations, the buoyancy of the artificial reef created vertical motion as the mooring lines stretched, pre-tensioning the components. The static simulation results in tension and heave for the reef system are shown in Figure 4.

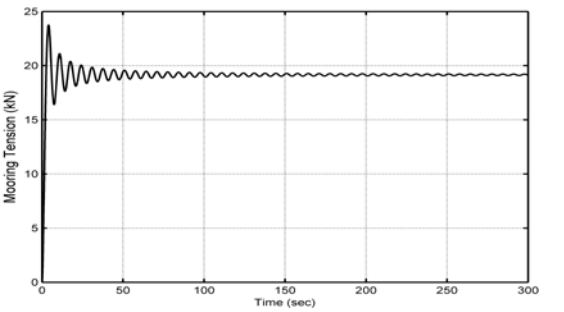

(a)

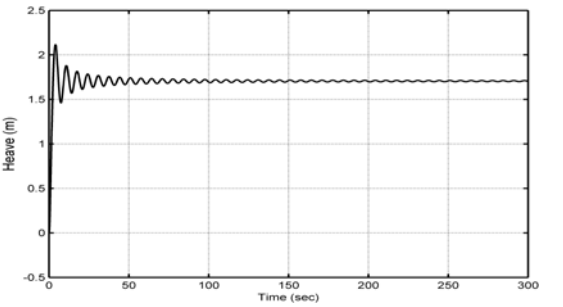

(b)

Figure 4: Static response of the pipe reef system in tension (a) and heave (b).

3.2 Dynamic results in regular waves

Recall, that the motion response was reported for the bottom of the buoy holder(nodes 3 and 4). As shown on the plots, the transient portion of the

simulation became steady at approximately 100 sec(1000 data points). The average values in tension, heave, surge and pitch for each of the load cases are provided in Table 5. Using the approach described for regular wave tests, the tension and motion RAO values were calculated and are provided in Table 6. It must be noted the motions(especially heave and pitch) are likely coupled. In addition to the average and RAO values, maximum amplitude values are provided in Table 7. The transfer function results in tension and heave are provided in Figure 5.

Table 5: Average values for the pipe reef system.

Load case	Tension (N)	Heave (m)	Surge (m)	Pitch (rad)
1	18956	1.6876	0.1483	-0.0020
2	19007	1.6872	0.5226	-0.0125
3	19217	1.6953	0.8417	-0.0212
4	19716	1.7191	1.1797	-0.0302
5	-	-	-	-
6	19415	-1.1630	14.92	-0.3582
7	19771	-1.7227	16.3117	-0.3966
8	20141	-2.3615	17.7384	-0.4380
9	20640	-2.9432	18.9439	-0.4715

Table 6: RAOs for the pipe reef system normalized without the influence of currents.

Load case	RAOs			
	Tension (N/m)	Heave (m/m)	Surge (m/m)	Pitch (rad/rad)
1	5098	0.4541	0.1795	0.0980
2	4342	0.3897	0.2755	0.1150
3	3423	0.3141	0.3382	0.1938
4	2729	0.2548	0.3847	0.3564
5	-	-	-	-

Table 7: Maximum amplitude values for the pipe reef system.

Load case	Tension (N)	Heave (m)	Surge (m)	Pitch (rad)
6	21742	-0.9368	15.0280	-0.3398
7	26553	-0.9911	16.6120	-0.3655
8	29552	-1.1884	18.3020	-0.4000
9	31527	-1.3937	19.9350	-0.4219

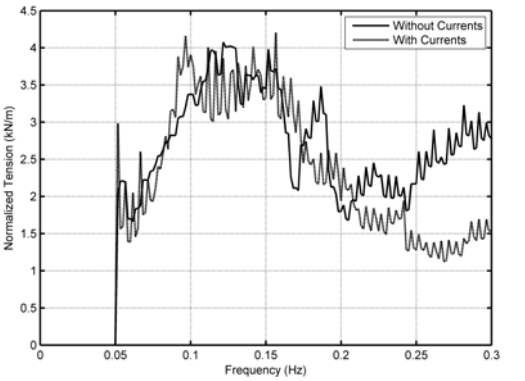

(a)

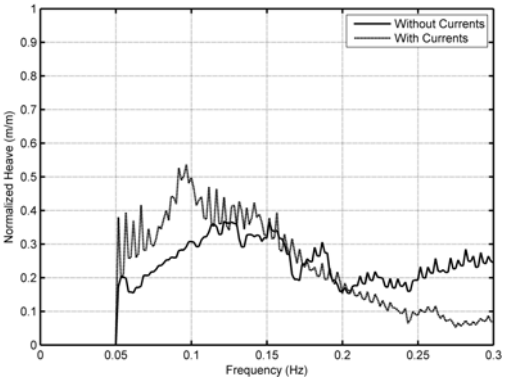

(b)

Figure 5: Transfer function results in tension (a) and heave (b) for the pipe reef system.

3.3 Dynamic results in irregular waves

Once the static and regular wave tests were completed, irregular wave tests were performed with and without the 1.0m/sec current. The time series generated by the numerical model was processed to obtain

the wave elevation auto-spectrum. The first step in analyzing the irregular wave results was to characterized tensions and motions by the zeroth moment of each spectral response using equations (7) and (8). The results for this calculation, called the significant response, are provided in Table 8 for the reef systems heave, surge and pitch and the mooring element tensions. The Tables show the response differences between the wave input with and without a 1.0 m/sec co-linear current. In addition, tension and heave spectral results for the pipe reef system are provided on Figures 6 and 7.

Table 8: Significant wave response values for the pipe reef system.

Current (m/sec)	Waves (m)	Tension (N)	Heave (m)	Surge (m)	Pitch (rad)
0	8.62	24752	2.27	3.70	0.100
1	8.62	24770	3.28	3.41	0.121

In addition to the "significant response" results, transfer functions were also calculated. The spectral representation of the wave input, motion response in heave, surge and pitch and the tension responses were calculated. The calculations were performed using equations (9) and (10) to obtain the wave elevation($G_{\eta\eta}$), heave(G_{hh}), surge(G_{ss}), pitch(G_{pp}) and mooring element tension(G_{tt}) response spectra. The input wave spectrum was used with equations (11) and (12) to calculate the wave excursion($G_{\xi\xi}$) and wave slope($G_{\theta\theta}$) spectra. The wave parameter input, the reef motion response and the mooring tension response spectra were used with equations (13), (14), (15) and (16) to obtain the heave, surge, pitch and mooring tension linear transfer functions. For the reef system transfer function results, the data sets were processed using a high-pass cutoff of 0.045 Hz.

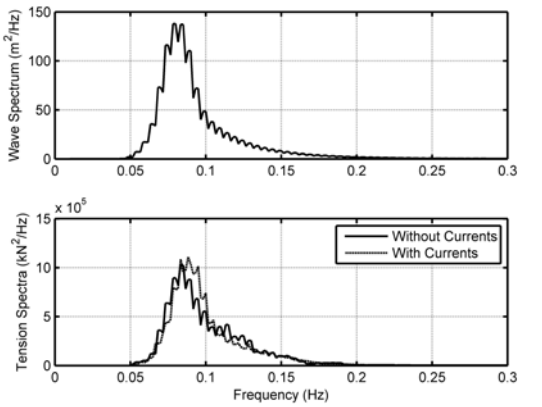

Figure 6: Surface elevation and tension spectral results for the pipe reef system.

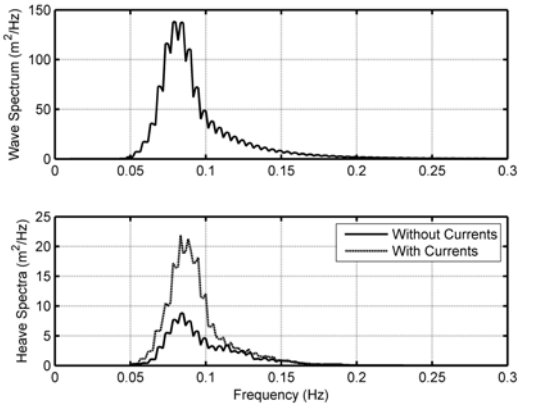

Figure 7: Surface elevation and heave spectral results for the pipe reef system.

Review of the dynamic simulations does not provide a strong indication of possible resonant conditions when subjected to the prescribed wave conditions. One of the most interesting results, however, of the

numerical model simulations were from the static tests. Typically, the model is built with a predetermined mooring line length, but since the mooring line is actually a spring, upon the initiation of the model run, the buoyancy of the reef component stretches the against the restoring force of the mooring line causing an oscillation. The static heave result shown in Figure 4(b) for the reef system was further investigated with details shown by the solid lines on Figure 8. The damped and natural periods of this oscillation were determined to examine if a resonating situation exists. Assuming an unforced, spring-mass system with linear damping, the system characteristics can be determined by solving the standard, second order, harmonic differential equation(note that the numerical model employs quadratic damping inherent in its formulation). The system characteristics including the damped natural period, undamped natural frequency, damping ratio, linear damping coefficient, spring constant and virtual mass values for the reef system are provided in Table 9. The results were then plotted on Figure 8 as the dashed line to show how the linear representation fit the numerical model results.

Review of the values provided in Table 9 and the plots shown on Figure 8 show systems with relatively little damping(in heave) with damped natural periods of 6.7 sec. This combination of system characteristics promotes a possible resonating situation in typical open ocean sea conditions with similar wave periods. Small damping values also indicate that oscillating amplitudes could be higher than expected.

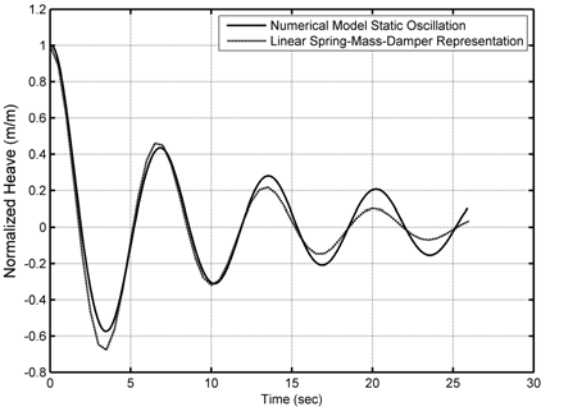

Figure 8: Normalized oscillation results of the pipe reef system.

Table 9: Oscillation response values of floating artificial reef with pipe.

Parameter	Values
Damped natural period(sec)	6.7
Undamped natural frequency(rad/sec)	0.944
Damping ratio(n/a)	0.114
Linear damping coefficient(N(m/sec)$^{-1}$)	2749
Spring constant(N/m)	11420
Virtual mass(kg)	12820

4. Conclusion

The mooring line tension and motion response results of a floating fish reef system with pipe were analyzed using a numerical model results. Using a Morison equation type model, simulations of the system were conducted. The first set of tests conducted with the reef system was performed with no forcing so that the static characteristics of each system were verified. The next set of tests was performed with the numerical model in regular and irregular waves(JONSWAP spectrum) with and without the 1.0m/sec

current. Heave, surge and pitch dynamic calculations were made, along with tension responses in the mooring line. The system has relatively little damping(in heave) with damped natural periods of 6.7 sec. This combination of system characteristics promotes a possible resonating situation in typical open ocean sea conditions with similar wave periods. Small damping values also indicate that oscillating amplitudes could be higher than expected.

Acknowledgements

This work was supported by the Korea Research Foundation Grant funded by the Korean Government(MOEHRD) (KRF-2007-313-F00073).

References

[1] Korean Ministry of Maritime Affairs and Fisheries, "Installation of artificial reef, pp. 1-5, 2007 (in Korean).

[2] C. G. Kim, H. S. Kim, T. H. Kim and C. I. Baik, "Monitoring of floating fish reef installed in Koje coastal waters", Ocean and Polar, vol. 23, no. 3, pp. 305-310, 2001.

[3] I. Tsukrov, O. Eroshkin, D. W. Fredriksson, M. R. Swift and B. Celikkol, "Finite element modeling of net panels using consistent net elements", Ocean Eng., vol. 30, pp. 251-270, 2003.

[4] I. Tsukrov, O. Eroshkin, W. Paul and B. Celikkol, "Numerical modeling of nonlinear elastic components of mooring systems", IEEE J. Oceanic Eng., vol. 30, no. 1, pp. 37-46, 2005.

[5] J. DeCew, D. W. Fredriksson, L. Bougrov, M. R. Swift, O. Eroshkin and B. Celikkol, " Numerical and physical modeling of a modified gravity type cage and mooring system", IEEE J. of Ocean. Eng., vol. 30, no. 1, pp. 47-58, 2005.

[6] D. W. Fredriksson, M. R. Swift, J. D. Irish, I. Tsukrov and B. Celikkol, "Fish cage and mooring system dynamics using physical and numerical models with field measurements", Aqua. Eng., vol. 27, no. 2, pp. 117-270, 2003.

[7] D. W. Fredriksson, M. R. Swift, J. D. Irish and B. Celikkol, "The heave response of a central spar fish cage", Transactions of the ASME, J. of Off. Mech. and Arct. Eng., vol. 25, pp. 242-248, 2003.

[8] D. W. Fredriksson, M. J. Palczynski, M. R. Swift and J. D. Irish, "Fluid dynamic drag of a central spar cage open ocean aquaculture IV, June 17-20, St. Andrews, NB, Canada, Mississippi-Alabama Sea Grant Consortium, Ocean Springs, MS. MASGP-01-006, 2001, 2003.

[9] D. W. Fredriksson, M. R. Swift, O. Eroshkin, I. Tsukrov, J. D. Irish and B. Celikkol, "Moored fish cage dynamics in waves and currents", Special issue on open ocean aquaculture engineering. IEEE J. Oceanic. Eng., vol. 30, no. 1, pp. 28-36, 2005.

[10] D. W. Fredriksson, I. Tsukrov, K. Baldwin, M. R. Swift and B. Celikkol, "Open ocean fish cage and mooring system modeling", Fisheries Dynamics 2003, National Fisheries Research and Devlopement Institute, Busan S. Korea. pp. 109-122, 2003.

[11] J. R. Morison, J. W. Johnson, M. P.

O'Brien and S. A. Schaaf, "The forces exerted by surface waves on piles", Petroleum Transactions, American Inst. of Mining Eng., pp. 149-157, 1950.
[12] N. Haritos and D. T. He, "Modelling the response of cable elements in an ocean environment", Fin. Elem. in Analysis and Des., vol. 19, pp. 19-32, 1992.
[13] Y. Goda, "Random seas and the design of maritime structures. World Scientific Publishing Company, New Jersey. 443p, 2000.
[14] www.kordi.re.kr
[15] M. K. Ochi, "Ocean waves: The stochastic approach", Cambridge University Press, New York, 1998.
[16] Shore Protection Manual, 4th ed., 2 Vols., US Army Engineer Waterways Experiment Station, Coastal Engineering Research Center, US Government Printing Office, Washing, DC, 1984.

Author Profile

Tae-Ho Kim

He received the B. F. degree from Yosu National University and M.F. and Ph.D. degrees from Pukyong National University. He had been with National Fisheries Research and Development Institute as a researcher and senior researcher. He is currently a associate professor in the School of Marine Technology at Chonnam National University.